IEEE Access
Multidisciplinary | Rapid Review | Open Access Journal

Received November 14, 2020, accepted November 27, 2020, date of publication December 1, 2020,
date of current version December 10, 2020.

Digital Object Identifier 10.1109/ACCESS.2020.3041680

Reliable and Secure Transmission in Multiple Antennas Hybrid Satellite-Terrestrial Cognitive Networks Relying on NOMA

HONG-NHU NGUYEN[1], NGOC-LONG NGUYEN[1], NHAT-TIEN NGUYEN[1], ANH-TU LE[2], NHAT-DUY XUAN HA[2], DINH-THUAN DO[3], (Senior Member, IEEE), AND MIROSLAV VOZNAK[1], (Senior Member, IEEE)

[1]Department of Telecommunications, VSB Technical University of Ostrava, 70833 Ostrava, Czech Republic
[2]Faculty of Electronics Technology, Industrial University of Ho Chi Minh City (IUH), Ho Chi Minh City 700000, Vietnam
[3]Department of Computer Science and Information Engineering, College of Information and Electrical Engineering, Asia University, Taichung 41354, Taiwan

Corresponding author: Dinh-Thuan Do (dodinhthuan@asia.edu.tw)

This work was supported by the Czech Ministry of Education, Youth and Sports conducted at the VSB - Technical University of Ostrava under Grant SP2020/65.

ABSTRACT We study a hybrid satellite-terrestrial cognitive network (HSTCN) relying on non-orthogonal multiple access (NOMA) interconnecting a satellite and multiple terrestrial nodes. In this scenario, the long distance communication is achieved by the satellite equipped multiple antennas to send information to a multi-antenna destinations through the base station acting as relay. The secure performance is necessary to study by exploiting the appearance of an eavesdropper attempting to intercept the transmissions from relay to destinations. We explore situation of hardware imperfections in secondary network and deign of multiple antennas need be investigated in term of the physical-layer security by adopting the decode-and-forward (DF) relay strategy. Specifically, we guarantee coverage area by enabling relaying scheme and keep outage probability (OP) performance satisfying required data rates. Moreover, suppose that only the main channels' state information is known while the wiretap channels' state information is unavailable due to the passive eavesdropper, we analyze the secrecy performance in term of intercept probability (IP) of the HSTCN by driving the closed-form expressions of such performance metric. Finally, the presented simulation results show that: *1) The outage behaviors of NOMA-based HSTCN network does not depend on transmit signal to noise ratio (SNR) at source at high SNR; 2) Numerical results show that the such system using higher number of transceiver antennas generally outperform the system with less antennas in terms of OP and IP and reasonable selection of parameters is necessary to remain the secrecy performance of such systems; and 3) By allocating different power levels to tow users, the second user has better secure behavior compared with the first user regardless of other set of satellite links or the number of antennas, which means that the superiority of the second user compared with user the first user in terms of OP and IP are same.*

INDEX TERMS Hybrid satellite-terrestrial cognitive systems, outage probability, Shadowed-Rician fading.

I. INTRODUCTION

To provide advances such as navigation assistance, ubiquitous large coverage and fast services in disaster areas, land mobile satellite (LMS) communication systems benefit to deployment of future wireless networks [1]. Besides these advantages, LMS systems meet the major challenges such as the masking effect due to nonexistence of a direct line-of-sight (LoS) link between the satellite and terrestrial user equipments (UEs) related to heavy rain, fog attenuation and/or poor angles [2]. In particular, the low-power and low-cost terrestrial UEs located in a tunnel or a building meet difficulties to send information to the satellite due to limited transmit power. A hybrid terrestrial-satellite relaying communications have has been recommended in [3]–[5] to overcome the effect of masking. Since then, such system has attracted a significant amount of works. For instance, in [3], the authors studied the impact of co-channel

The associate editor coordinating the review of this manuscript and approving it for publication was Mohammad Tariqul Islam.

interference (CCI) from the terrestrial network for the context of amplify-and-forward (AF) protocol deployed at the terrestrial relay. More importantly, they derived the approximate statistical distributions signal-to-interference-plus noise ratio (SINR) and hence exhibited some asymptotical computations of bit-error rate (BER) as main evaluation for the system performance. To obtain more insights into the system performance. Later, a hybrid satellite-terrestrial relay system employing multiple amplify-and-forward relays was explored by further exploiting a multi-antenna satellite to communicate with multiple users [4]. A max-max user-relay selection approach is provided to minimize the outage probability of the considered system [4]. The authors in [5] presented the average symbol error rate (SER) and obtained expression of the diversity order in the considered network in which technique for channel estimation and detection of transmitted signal are adopted related transmission between the terrestrial UE and the satellites. Moreover, the authors in [6] examined performance of AF hybrid terrestrial-satellite relaying networks with opportunistic Scheduling by deriving expressions in term of the ergodic capacity.

Actually, raised issues need be studied due to the challenges of low spectrum resource utilization and high cost in implementation of satellite mobile users [7]. As a model of cognitive radio (CR), spectrum sharing among satellite and terrestrial networks is known as promising candidate to design hybrid satellite-terrestrial cognitive networks (HSTCNs) [8]–[10]. By looking at the requirements of both spectrum efficiency and reliability, HSTCN can provide comprehensive wireless coverage as well as improve spectrum resource usage. The authors in [10] provided the closed-form formula of the outage probability (OP) for the considered system in the presence of interference power constraints imposed by multiple adjacent terrestrial primary users (PUs). The authors in [11] studied the interweave architecture for HSTCN to allow the satellite share idle spectrum with terrestrial networks. They indicated that cognitive satellite systems can not only improve the spectrum utilization but also benefit their operational revenues. However, finding out the realtime idle spectrum is difficult task for the terrestrial networks. To this end, the underlay paradigm recommended in HSTCNs as [12], [13], which, however, would cause unavoidable CCI among secondary users (SUs) and primary users (PUs). Therefore, as further difficult task due to the unknown of channel state information (CSI) exchange, a key issue regarding reliable coordination between satellite and terrestrial networks has become necessary open problems. Reference [2] addressed its achievable rate maximization. They first converted the CCI threshold into transmit power constraints, and then formulate the maximization of the achievable rate as an optimization problem. The authors in [14] explored the security problem for energy harvesting-assisted cognitive satellite-terrestrial network containing a base station, some mobile users (MUs) and energy receivers (ERs), in which a multi-beam satellite sub-network shares the portion of millimeter wave bands with multiple cellular networks. The work in [15] considered system model to allow the secondary network selection to achieve optimal outage probability of the primary satellite system and then provide spectrum sharing opportunities.

As further paradigm providing spectrum efficiency for forthcoming networks, non-orthogonal multiple access (NOMA) [16]–[20] was investigated as promising wireless access technique. In principle, at the transmitter NOMA employs non-orthogonal transmission and users' superposed information achieved in power domain for higher spectrum efficiency. NOMA can serve multiple users over the same resource block, which is different from traditional orthogonal multiple access (OMA) [21], [22] and hence it can effectively improve sum rate. At the receiver, Successive Interference Cancellation (SIC) is implemented to decode the users' information. Specifically, by considering other users as interference the user with the best channel condition can be decoded firstly In [21], the authors studied the relaying scheme employed in the secondary network of the proposed CR-NOMA and the relay can be harvest energy from the secondary transmitter to serve signal forwarding to distant secondary users. They considered the complex model of wireless powered CR-NOMA in terms of outage behavior and throughput performance as awareness on imperfect SIC at the receiver. The authors [22] examined the secondary users (SUs) in the CR-NOMA network opportunistically access the licensed spectrum resources to foster the number of accessible SUs sharing the limited and dynamic spectrum resources. Moreover, partial relay selection architecture is exploited at full-duplex (FD) and half duplex (HD) relays to enhance the performance of far users. Reference [23]–[26] introduced lots of scenarios of CR-NOMA systems along with the system performance analysis. For example, [24] designed a CR-NOMA model and an spectrum efficiency optimization problem which was solved by optimizing the sensing sub-slot. Since CR-NOMA combines the advantages of the energy harvesting and device-to-device transmission mode, it is considered as a promising approach for the coming 5G communication system [25], [26].

The authors in [8], [27], [28] investigated benefits of NOMA in HSTCN. For example, [27] explored the performance of an underlay cognitive hybrid satellite-terrestrial network comprising a primary satellite source with its terrestrial receiver and the secondary transmitter (ST) with its pre-paired users on the ground. Particularly, the ST uses a cooperative NOMA scheme to permit a nearby NOMA user operating as a relay and detects and forwards signals to the distant NOMA user during the cooperation phase. Reference [8] investigated the outage probability (OP) performance of amplify-and-forward (AF) HSTCN with the NOMA scheme. In such, half-duplexing terrestrial secondary networks cooperate with a primary satellite network to provide dynamic spectrum access. By adopting pertinent heterogeneous fading models the authors in [28] obtained the closed-form expressions for the OP of primary satellite network and secondary terrestrial network. Further, we derived

the asymptotic outage behavior at high signal-to-noise-ratio (SNR) for the primary and secondary networks, and thereby calculated the achievable diversity orders.

A. RELATED WORK AND MOTIVATION

The authors in [29] proposed beamforming (BF) schemes to utilize the interference from the terrestrial network as a green source to improve the physical-layer security for the HSTRN network, provided that the two networks share the portion of millimeter-wave frequencies. In [30], HSTRN system is studied in the situation that the satellite sends information to a destination through multiple relays at the existence of an eavesdropper attempting to intercept the transmissions from both the satellite and relays. They explored the context of the single-relay selection and multi-relay selection as well as round-robin scheduling schemes to address the physical-layer security of this considered HSTRN by adopting the decode-and-forward (DF) relay scheme. Reference [31] investigated the secure transmission for HSTRN where the terrestrial base station serving as a green interference resource to enhance the security of the satellite link. The authors adopted a stochastic model for the channel state information uncertainty and proposed a secure and robust beamforming framework to minimize the transmit power, while satisfying a range of outage (probabilistic) constraints at the satellite user and the terrestrial user.

However, they only considered the secure transmission for HSTRN. To the best of our knowledge, there is no prior work consider secure performance of NOMA-HSTCNs in the contexts of multiple-antenna and cooperative spectrum sharing. Therefore, we explore outage performance and secure performance metric for such systems.

B. OUR CONTRIBUTION AND ORGANIZATION

The detailed contributions of this paper are outlined as follows:

- This framework is different from the system models of [29]–[31]. In particular, we experience the practical situation that the eavesdropper is able to intercept from only the terrestrial network. More specifically, we propose a practical framework of physical layer security in a NOMA-HSTCN containing nodes with hardware impairments. In such, we design one satellite to communicate to two terrestrial destination through terrestrial relay at the existence of one terrestrial eavesdropper.
- We present analytical expressions to indicate two important performance metrics such as the outage probability (OP) and intercept probability of the such system, which is applicable to evaluate reliable and secure transmission of such NOMA-HSTCN which benefits from design of multiple-antenna.
- To provide further insight, we show trends of for OP and IP at high SNR region. This is interesting guidelines to configure such system in practice. Then, we indicate which parameters are used to improve performance of specific user to satisfy specific demands in the context of NOMA.
- To provide details of our contribution, we summarize main advances in Table 1 which indicates some achieved improvements compared with other recent studies.

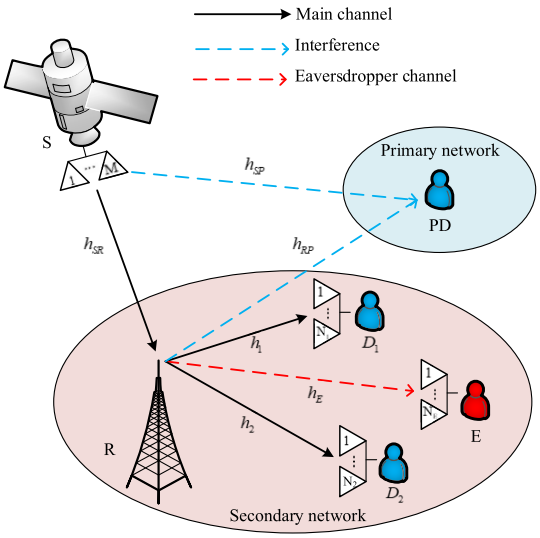

FIGURE 1. System model of NOMA-HSTCN networks.

The remainder of the paper is organized as follows. Section II provides details of the system model. In Section III, closed-form expressions of OP and IP are provided. In Section IV presents numerical results and discussion. Finally, Section V provides some concluding remarks along with future research directions.

II. SYSTEM MODEL

As depicted in Fig. 1, we consider the secondary network of the NOMA-HSTCN which consists a base station (S) facilitated M antenna, a relay (R) adopted half-duplex along with decode-and-forward (DF) protocol. It is noted that relay equipped single antenna due to low-cost and limited power, two destinations D_i with N_i antennas, a eavesdropper (E) with N_E antennas. In primary network, we assumed the primary destination (PD) equipped single antenna has significant impacts from secondary network. Furthermore, we assume no direct link between S and D_i [32] due to obstructions. Then, the transmit signal of S is given as

$$x_S = \sqrt{P_S}\left(\sqrt{a_1}x_1 + \sqrt{a_2}x_2\right). \tag{1}$$

In the first phase, S transmits the signal x_S to relay R. Thus, the received signal at R is given as

$$\begin{aligned} y_R &= \mathbf{h}_{SR}^{\dagger}\mathbf{w}_{SR}\left[x_S + \eta_{SR}\right] + n_R \\ &= \mathbf{h}_{SR}^{\dagger}\mathbf{w}_{SR}\left[\sqrt{P_S}\left(\sqrt{a_1}x_1 + \sqrt{a_2}x_2\right) + \eta_{SR}\right] + n_R. \end{aligned} \tag{2}$$

According to the principle of maximum ratio transmission (MRT) [4], $\mathbf{w}_{SR} = \frac{\mathbf{h}_{SR}}{\|\mathbf{h}_{SR}\|_F}$. The signal to interference plus

TABLE 1. Comparison of proposed system with related works.

Context	Cooperative Relay Network	Relay Protocol	NOMA	Cognitive Radio	Intercept Probability	Diversity order	Hardware Impairments
Our Work	Yes	DF	Yes	Yes	Yes	Yes	Yes
[34]	Yes	DF	No	No	No	No	Yes
[40]	Yes	AF	No	No	No	No	Yes
[41]	Yes	AF	Yes	No	No	Yes	No
[42]	Yes	DF	Yes	No	No	Yes	No
[43]	Yes	DF	No	No	No	Yes	No

TABLE 2. The symbols in considered systems.

Symbol	Description
x_S	The signal of base station
x_R	The signal of relay
$x_i (i \in \{1,2\})$	The signal of D_i
P_S	The transmit power at base station
P_R	The transmit power at relay
P_P	The transmit power at primary destination
$\bar{P}_S$	The maximum available transmit power at base station
$\bar{P}_R$	The maximum available transmit power at relay
a_i and b_i	The power allocation coefficients with $a_1 + a_2 = 1$, $b_1 + b_2 = 1$, $a_2 > a_1$ and $b_2 > b_1$
η_{SR}, η_{RD_i} and η_E	The distortion noise caused by hardware impairments (HIs) with $\mathcal{CN}\left(0, P_R k_{SR}^2\right)$, $\mathcal{CN}\left(0, P_R k_{RD_i}^2\right)$ and $\mathcal{CN}\left(0, P_R k_E^2\right)$ respectively
n_R, $\mathbf{n}_i$ and $\mathbf{n}_E$	The additive white Gaussian noise (AWGN) with $\mathcal{CN}\left(0, \sigma_R^2\right)$, $\mathcal{CN}\left(0, \sigma_i^2\right)$ and $\mathcal{CN}\left(0, \sigma_E^2\right)$ respectively
k_u^2	the level of hardware impairments related to link u [42]
$\mathbf{w}_{SR}$	The transmit beamforming vector
$\mathbf{w}_{RD_i}$ and $\mathbf{w}_E$	The received beamforming vector
$\mathbf{h}_{SR}$	The channel vector from base station to relay
$\mathbf{h}_{SP}$	The channel vector from base station to primary destination
$\mathbf{h}_{RD_i}$	The channel vector from relay to D_i
$\mathbf{h}_E$	The channel vector from relay to E
h_{RP}	The channel from relay to primary destination

noise ratio (SINR) to detect signal x_2 at R is given by

$$\gamma_{R,x_2} = \frac{P_S a_2 \mathcal{H}_{SR}}{P_S a_1 \mathcal{H}_{SR} + P_S k_{SR}^2 \mathcal{H}_{SR} + \sigma_R^2}, \tag{3}$$

where $\mathcal{H}_j = \left\|\mathbf{h}_j\right\|_F^2$ with $j \in \{SR, SP\}$. Further, the SINR to detect x_1 at R is given by

$$\gamma_{R,x_1} = \frac{P_S a_1 \mathcal{H}_{SR}}{P_S k_{SR}^2 \mathcal{H}_{SR} + \sigma_R^2}. \tag{4}$$

Due interference constraint, it is necessary to limit interference of the PD being beyond an acceptable level P_P, the transmit power at S and R are given as respectively [33]

$$P_S = \min\left(\bar{P}_S, \frac{P_P}{\mathcal{H}_{SP}}\right), \tag{5}$$

and

$$P_R = \min\left(\bar{P}_R, \frac{P_P}{|h_{RP}|^2}\right). \tag{6}$$

In the second phase, the relay employs DF protocol and transmits the information $x_R = \sqrt{P_R}(\sqrt{b_1}x_1 + \sqrt{b_2}x_2)$ to D_i and E. Then, the received signal at D_i and E are given respectively by

$$\begin{aligned} y_{D_i} &= \mathbf{h}_{RD_i}\mathbf{w}_{RD_i}^\dagger\left[x_R + \eta_{RD_1}\right] + \mathbf{w}_{RD_i}^\dagger \mathbf{n}_i \\ &= \mathbf{h}_{RD_i}\mathbf{w}_{RD_i}^\dagger \\ &\quad \times \left[\sqrt{P_R}\left(\sqrt{b_1}x_1 + \sqrt{b_2}x_2\right) + \eta_{RD_1}\right] + \mathbf{w}_{RD_i}^\dagger \mathbf{n}_i, \end{aligned} \tag{7}$$

and

$$\begin{aligned} y_E &= \mathbf{h}_E \mathbf{w}_E^\dagger\left[x_R + \eta_E\right] + \mathbf{w}_E^\dagger \mathbf{n}_E \\ &= \mathbf{h}_E \mathbf{w}_E^\dagger\left[\sqrt{P_R}\left(\sqrt{b_1}x_1 + \sqrt{b_2}x_2\right) + \eta_E\right] + \mathbf{w}_E^\dagger \mathbf{n}_E. \end{aligned} \tag{8}$$

Based on the maximal-ratio combining (MRC) scheme [35], we have $\mathbf{w}_{RD_i} = \frac{\mathbf{h}_{RD_i}}{\left\|\mathbf{h}_{RD_i}\right\|_F}$. Then, the SINR to detect x_2 at D_2 is given as

$$\gamma_{D_2,x_2} = \frac{P_R b_2 \mathcal{H}_{RD_2}}{P_R b_1 \mathcal{H}_{RD_2} + P_R k_{RD_2}^2 \mathcal{H}_{RD_2} + \sigma_2^2}, \tag{9}$$

where $\mathcal{H}_i = \left\|\mathbf{h}_{RD_i}\right\|_F^2$. Moreover, the SINR to detect the signal x_2 at D_1 is given as

$$\gamma_{D_1,x_2} = \frac{P_R b_2 \mathcal{H}_{RD_1}}{P_R b_1 \mathcal{H}_{RD_1} + P_R k_{RD_1}^2 \mathcal{H}_{RD_1} + \sigma_1^2} \tag{10}$$

Applying SIC, the SINR at D_1 to detected the own signal x_1 is given as

$$\gamma_{D_1,x_1} = \frac{P_R b_1 \mathcal{H}_{RD_1}}{P_R k_{RD_1}^2 \mathcal{H}_{RD_1} + \sigma_1^2} \tag{11}$$

According to the NOMA principle, E successfully eliminates the signal x_2 and treats the signal x_1 as noise. Then, we can obtain as

$$\gamma_{E,x_2} = \frac{P_R b_2 \mathcal{H}_E}{P_R b_1 \mathcal{H}_E + P_R k_E^2 \mathcal{H}_E + \sigma_E^2} \tag{12}$$

where $\mathcal{H}_E = \|\mathbf{h}_E\|_F^2$. Moreover, E successfully eliminates the signal x_1 of D_1 with SIC. Thus, we can obtain as

$$\gamma_{E,x_1} = \frac{P_R b_1 \mathcal{H}_E}{P_R k_E^2 \mathcal{H}_E + \sigma_E^2} \tag{13}$$

III. PERFORMANCE ANALYSIS

As most of research on physical layer security, a couple of common criterion to characterize the secrecy performance are secure outage probability (SOP) and intercept probability (IP).[1] Therefore, we measure the OP and IP performance, which provide important guidelines to deploy such NOMA-HSTCN systems.

A. CHANNEL MODEL

First, we assume the channel vector h_j independent and identically distributed (i.i.d.) Shadowed-Rician fading. Moreover, the probability density function (PDF) of $h_j^{(k)}$ with satellites' k-th antenna is computed by [4]

$$f_{\left|h_j^{(k)}\right|^2}(x) = \alpha_j e_1^{-\beta_j x} F_1\left(m_j; 1; \delta_j x\right), \quad x > 0, \tag{14}$$

where m_j are the fading severity parameter, Ω_j and $2b_j$ are the average power of LOS and multi-path components, respectively, $\alpha_j = (2b_j m_j/(2b_j m_j + \Omega_j)^{m_j}/2b_j$, $\beta_j = 0.5b_j$, $\delta_j = \Omega_j/(2b_j)(2b_j m_j + \Omega_j)$ and ${}_1F_1(\cdot;\cdot;\cdot)$ is the confluent hypergeometric function of the first kind [45, Eq. 9.210.1]. Moreover, with m_j is an integer number (14) is rewritten as

$$f_{\left|h_j^{(k)}\right|^2}(x) = \alpha_j \sum_{kj=0}^{m_j-1} \zeta_j\left(k_j\right) x^{k_j} e^{-(\beta_j-\delta_j)x} \tag{15}$$

where $\zeta_j(\ell) = (-1)^\ell \left(1-m_j\right)_\ell \delta_j^\ell/(\ell!)^2$, $(.)_\ell$ is the Pochhammer symbol [45, p.xliii]. Thus, the PDF of $\mathcal{H}_j$ is given as

$$f_{\mathcal{H}_j}(x) = \sum_{i_1=0}^{m_j-1} \cdots \sum_{i_M=0}^{m_j-1} \Theta(j, M) x^{\Delta_j - 1} e^{-(\beta_j-\delta_j)x}, \tag{16}$$

where $\Theta(j, M) = \alpha_j^M \prod_{\ell=1}^M \zeta_j(i_\ell) \prod_{j=1}^{M-1} ß(\sum_{l=1}^j i_l + j, i_{j+1} + 1)$, $\Delta_j = \sum_{q=1}^M i_q + M$ and $ß(.,.)$ is the Beta function.

Regarding channels in ground, the PDF of $|h_{RP}|^2$ is given as

$$f_{|h_{RP}|^2}(x) = \frac{x^{m_{RP}-1}}{\Gamma(m_{RP})\Lambda_{RP}^{m_{RP}}} e^{-\frac{x}{\Lambda_{RP}}}, \tag{17}$$

where $\Lambda = \frac{\lambda}{m}$, m and Ω are present the fading severity factor and mean, respectively.

[1] In this paper, we want to evaluate reliable characteristic with outage probability rather than considering SOP, which is reported a lot in the literature, for example in [34].

Moreover, the PDF of $\mathcal{H}_v$ in which $v \in \{1, 2, E\}$ are given as respectively [36]

$$f_{\mathcal{H}_v}(x) = \frac{x^{N_v m_v - 1}}{\Gamma(N_v m_v)\Lambda^{N_v m_v}} e^{-\frac{x}{\Lambda_v}}. \tag{18}$$

B. OUTAGE PROBABILITY

1) OUTAGE PROBABILITY OF D_1

The outage probability is evaluated as ability to a user detect its signal at related nodes. In this manner, signal x_1 of user of D_1 is processed at relay and destination D_1. Such outage probability at D_1 is expressed as

$$\begin{aligned} P_{D_1}^{out} &= \Pr\left(\min\left(\gamma_{R,x_1}, \gamma_{D_1,x_1}\right) < \gamma_{th_1}\right) \\ &= 1 - \underbrace{\Pr\left(\gamma_{R,x_1} > \gamma_{th_1}\right)}_{A_1} \underbrace{\Pr\left(\gamma_{D_1,x_1} > \gamma_{th_1}\right)}_{A_2}, \end{aligned} \tag{19}$$

where $\gamma_{th_1} = 2^{2R_1} - 1$ and R_i is the target rates for user D_i.

Proposition 1: The component of overall OP, A_1 can be obtained as (20), as shown at the bottom of the page.

Proof: See Appendix A.

Proposition 2: The second term of (19) an be calculated as

$$\begin{aligned} A_2 = &\frac{\gamma\left(m_{RP}, \frac{\rho_D}{\Lambda_{RP}\bar{\rho}_R}\right)\Gamma\left(N_1 m_1, \frac{\bar{\phi}_1}{\bar{\rho}_R \Lambda_1}\right)}{\Gamma(m_{RP})\Gamma(N_1 m_1)} \\ &+ \sum_{p_2=0}^{N_1 m_1 - 1} \frac{(\Lambda_1\rho_D)^{m_{RP}}\left(\bar{\phi}_1\Lambda_{RP}\right)^{p_2}}{p_2!\Gamma(m_{RP})\left(\bar{\phi}_1\Lambda_{RP} + \Lambda_1\rho_D\right)^{m_{RP}+p_2}} \\ &\times \Gamma\left(m_{RP} + p_2, \frac{\bar{\phi}_1\Lambda_{RP} + \Lambda_1\rho_D}{\Lambda_1\bar{\rho}_R\Lambda_{RP}}\right). \end{aligned} \tag{21}$$

Proof: See Appendix B.

Finally, the closed-form expression for the OP of user D_1 is given by

$$P_{D_1}^{out} = 1 - A_1 \times A_2. \tag{22}$$

2) OUTAGE PROBABILITY OF D_2

It is worth noting that signal x_2 is detected at user D_1, and hence OP of user D_2 can be characterized by evaluating related SINRs compared with the thresholds. Therefore, the OP of user D_2 can be formulated by

$$\begin{aligned} P_{D_2}^{out} &= \Pr\left(\min\left(\gamma_{R,x_2}, \gamma_{D_2,x_2}, \gamma_{D_1,x_2}\right) < \gamma_{th_2}\right) \\ &= 1 - \underbrace{\Pr\left(\gamma_{R,x_2} > \gamma_{th_2}\right)}_{B_1} \underbrace{\Pr\left(\gamma_{D_2,x_2} < \gamma_{th_2}\right)}_{B_2} \\ &\quad \times \underbrace{\Pr\left(\gamma_{D_1,x_2} < \gamma_{th_2}\right)}_{B_3}. \end{aligned} \tag{23}$$

$$\begin{aligned} A_1 = &\widetilde{\sum}\left(m_{SR}, m_{SP}\right) \frac{(\beta_{SP} - \delta_{SP})^{-\Delta_{SP}}}{(\beta_{SR} - \delta_{SR})^{\Delta_{SR}}} \gamma\left(\Delta_{SP}, \frac{\rho_D(\beta_{SP} - \delta_{SP})}{\bar{\rho}_S}\right)\Gamma\left(\Delta_{SR}, \frac{\phi_1(\beta_{SR} - \delta_{SR})}{\bar{\rho}_S}\right) \\ &+ \widetilde{\sum}\left(m_{SR}, m_{SP}\right) \sum_{p_1=0}^{\Delta_{SR}-1} \frac{\Gamma(\Delta_{SR})\phi_1^{p_1}\rho_D^{\Delta_{SP}}\Gamma\left(\Delta_{SP} + p_1, \frac{(\beta_{SP}-\delta_{SP})\rho_D + (\beta_{SR}-\delta_{SR})\phi_1}{\bar{\rho}_S}\right)}{p_1!(\beta_{SR} - \delta_{SR})^{\Delta_{SR}-p_1}\left((\beta_{SP} - \delta_{SP})\rho_D + (\beta_{SR} - \delta_{SR})\phi_1\right)^{\Delta_{SP}+p_1}} \end{aligned} \tag{20}$$

Proposition 3: The closed-form expression of B_1 is given as (24), as shown at the bottom of the page.

Proof: With the help of (3), B_1 is written as

$$B_1 = \Pr\left(\mathcal{H}_{SP} < \frac{\rho_D}{\bar{\rho}_S}, \mathcal{H}_{SR} > \frac{\varphi_2}{\bar{\rho}_S}\right) + \Pr\left(\mathcal{H}_{SP} > \frac{\rho_D}{\bar{\rho}_S}, \mathcal{H}_{SR} > \frac{\varphi_2 \mathcal{H}_{SP}}{\rho_D}\right), \quad (25)$$

where $\varphi_2 = \frac{\gamma_{th_2}}{(a_2 - a_1\gamma_{th_2} - k_{SR}^2\gamma_{th_2})}$. It then can be rewritten by

$$B_1 = \int_0^{\frac{\rho_D}{\bar{\rho}_S}} f_{\mathcal{H}_{SP}}(x) \int_{\frac{\varphi_2}{\bar{\rho}_S}}^{\infty} f_{\mathcal{H}_{SR}}(y) dy dx + \int_{\frac{\rho_D}{\bar{\rho}_S}}^{\infty} f_{\mathcal{H}_{SP}}(x) \int_{\frac{\varphi_2 x}{\rho_D}}^{\infty} f_{\mathcal{H}_{SR}}(y) dy dx. \quad (26)$$

Similar in appendix A, (24) is obtained. The proof is completed.

Then, putting (9) into (23) we can write B_2 as

$$\begin{aligned} B_2 &= \Pr\left(|h_{RP}|^2 < \frac{\rho_D}{\bar{\rho}_S}, \mathcal{H}_{RD_2} > \frac{\bar{\varphi}_2}{\bar{\rho}_S}\right) + \Pr\left(|h_{RP}|^2 > \frac{\rho_D}{\bar{\rho}_S}, \mathcal{H}_{RD_2} > \frac{\bar{\varphi}_2 |h_{RP}|^2}{\rho_D}\right) \\ &= \int_0^{\frac{\rho_D}{\bar{\rho}_S}} f_{|h_{RP}|^2}(x) \int_{\frac{\bar{\varphi}_2}{\bar{\rho}_S}}^{\infty} f_{\mathcal{H}_{RD_2}}(y) dy dx + \int_{\frac{\rho_D}{\bar{\rho}_S}}^{\infty} f_{|h_{RP}|^2}(x) \int_{\frac{\bar{\varphi}_2 x}{\rho_D}}^{\infty} f_{\mathcal{H}_{RD_2}}(y) dy dx, \end{aligned} \quad (27)$$

where $\bar{\varphi}_2 = \frac{\gamma_{th_2}}{b_2 - \gamma_{th_2} b_1 - \gamma_{th_2} k_{RD_2}^2}$.

By performing similar computation, B_2, B_3 can be expressed respectively by

$$B_2 = \frac{\gamma\left(m_{RP}, \frac{\rho_D}{\Lambda_{RP}\bar{\rho}_R}\right)\Gamma\left(N_2 m_2, \frac{\bar{\varphi}_2}{\bar{\rho}_R \Lambda_2}\right)}{\Gamma(m_{RP})\Gamma(N_2 m_2)} + \sum_{p_3=0}^{N_2 m_2 - 1} \frac{(\Lambda_2\rho_D)^{m_{RP}} (\bar{\varphi}_2 \Lambda_{RP})^{p_3}}{p_3! \Gamma(m_{RP}) (\bar{\varphi}_2\Lambda_{RP} + \Lambda_2\rho_D)^{m_{RP}+p_3}} \times \Gamma\left(m_{RP} + p_3, \frac{\bar{\varphi}_2\Lambda_{RP} + \Lambda_2\rho_D}{\Lambda_2\bar{\rho}_R\Lambda_{RP}}\right), \quad (28)$$

$$B_3 = \frac{\gamma\left(m_{RP}, \frac{\rho_D}{\Lambda_{RP}\bar{\rho}_R}\right)\Gamma\left(N_1 m_1, \frac{\bar{\varphi}_2}{\bar{\rho}_R \Lambda_1}\right)}{\Gamma(m_{RP})\Gamma(N_1 m_1)} + \sum_{p_4=0}^{N_1 m_1 - 1} \frac{(\Lambda_1\rho_D)^{m_{RP}} (\bar{\varphi}_2 \Lambda_{RP})^{p_4}}{p_4! \Gamma(m_{RP}) (\bar{\varphi}_2\Lambda_{RP} + \Lambda_1\rho_D)^{m_{RP}+p_4}} \times \Gamma\left(m_{RP} + p_4, \frac{\bar{\varphi}_2\Lambda_{RP} + \Lambda_1\rho_D}{\Lambda_1\bar{\rho}_R\Lambda_{RP}}\right). \quad (29)$$

Then, we can compute OP for user D_2 as below

$$P_{D_2}^{out} = \begin{cases} 1 - B_1 \times B_2 \times B_3, & \text{if : } \gamma_{th_2} < \frac{b_2}{b_1 + k_{RD_2}^2} \\ & \gamma_{th_2} < \frac{a_2}{a_1 + k_{RD_2}^2} \\ 1, & \text{otherwise} \end{cases} \quad (30)$$

C. DIVERSITY ORDER ANALYSIS

In this paper, we consider asymptotic at high SNR. It is worth noting that the diversity order for D_1, D_2 are defined by

$$d = -\lim_{\bar{\rho}\to\infty} \frac{\log\left(P_{D_i}^{out,\infty}(\bar{\rho})\right)}{\log\bar{\rho}}. \quad (31)$$

When $\bar{\rho} \to \infty$, we apply a series representation of the incomplete Gamma function [45, Eq. 8.354.1] we have

$$\gamma(m, x) \overset{x\to 0}{\approx} \frac{x^m}{m}. \quad (32)$$

Then, we can write $P_{D_1}^{out,\infty}$ as (33), as shown at the bottom of the next page.

Next, $P_{D_2}^{out,\infty}$ is written as

$$P_{D_2}^{out} = 1 - B_1^{\infty} \times B_2^{\infty} \times B_3^{\infty}, \quad (34)$$

where B_1^{∞} is express as (35), as shown at the bottom of the next page. Hence, B_2^{∞} and B_3^{∞} are given in the bottom of the next page, respectively.

Therefore, the diversity orders of D_1 and D_2 are equal zero.

D. INTERCEPT PROBABILITY ANALYSIS

1) INTERCEPT PROBABILITY OF D_1

The intercept probability of D_1 is expressed as [37]

$$IP_{D_1}^{out} = \Pr\left(\gamma_{R,x_1} > \gamma_{th_1}, \gamma_{R,x_2} > \gamma_{th_2}, \gamma_{E,x_1} > \gamma_{E_1}\right) \quad (38)$$

where γ_{E_i} is the secrecy SNR threshold of D_i.

Proposition 4: The closed-form expression for IP of D_1 is given as (39), as shown at the bottom of the next page.

$$B_1 = \widetilde{\sum}(m_{SR}, m_{SP}) \frac{(\beta_{SP} - \delta_{SP})^{-\Delta_{SP}}}{(\beta_{SR} - \delta_{SR})^{\Delta_{SR}}} \gamma\left(\Delta_{SP}, \frac{\rho_D(\beta_{SP} - \delta_{SP})}{\bar{\rho}_S}\right) \Gamma\left(\Delta_{SR}, \frac{(\beta_{SR} - \delta_{SR})\varphi_2}{\bar{\rho}_S}\right) + \widetilde{\sum}(m_{SR}, m_{SP}) \sum_{p_3=0}^{\Delta_{SR}-1} \frac{\Gamma(\Delta_{SR}) \varphi_2^{p_3} \rho_D^{\Delta_{SP}} \Gamma\left(\Delta_{SP} + p_3, \frac{(\beta_{SP} - \delta_{SP})\rho_D + (\beta_{SR} - \delta_{SR})\varphi_2}{\bar{\rho}_S}\right)}{p_3! (\beta_{SR} - \delta_{SR})^{\Delta_{SR} - p_3} ((\beta_{SP} - \delta_{SP})\rho_D + (\beta_{SR} - \delta_{SR})\varphi_2)^{\Delta_{SP} + p_3}} \quad (24)$$

Proof: Putting (3), (4) and (5) into (39), we get (40)

$$IP_{D_1}^{out} = \Bigg[\underbrace{\Pr\left(\mathcal{H}_{SP} < \frac{\rho_D}{\bar{\rho}_S}, \mathcal{H}_{SR} > \frac{\eta}{\bar{\rho}_S}\right)}_{C_1} + \underbrace{\Pr\left(\mathcal{H}_{SP} > \frac{\rho_D}{\bar{\rho}_S}, \mathcal{H}_{SR} > \frac{\eta \mathcal{H}_{SP}}{\rho_D}\right)}_{C_2}\Bigg] \times \Bigg[\underbrace{\Pr\left(|h_{RP}|^2 < \frac{\rho_D}{\bar{\rho}_R}, \mathcal{H}_E > \frac{\bar{\phi}_3}{\bar{\rho}_R}\right)}_{C_3} + \underbrace{\Pr\left(|h_{RP}|^2 > \frac{\rho_D}{\bar{\rho}_R}, \mathcal{H}_E > \frac{\bar{\phi}_3 |h_{RP}|^2}{\rho_D}\right)}_{C_4}\Bigg], \quad (40)$$

$$P_{D_1}^{out,\infty} = 1 - \left(\widetilde{\sum} (m_{SR}, m_{SP}) \frac{(\beta_{SP} - \delta_{SP})^{-\Delta_{SP}}}{(\beta_{SR} - \delta_{SR})^{\Delta_{SR}} \Delta_{SP} \Delta_{SR}} \left(\frac{\rho_D (\beta_{SP} - \delta_{SP})}{\bar{\rho}_S}\right)^{\Delta_{SP}} \left(\Gamma(\Delta_{SR}+1) - \left(\frac{\phi_1 (\beta_{SR} - \delta_{SR})}{\bar{\rho}_S}\right)^{\Delta_{SR}}\right) + \widetilde{\sum} (m_{SR}, m_{SP}) \sum_{p_1=0}^{\Delta_{SR}-1} \frac{\Gamma(\Delta_{SR}) \phi_1^{p_1} \rho_D^{\Delta_{SP}} \left(\Gamma(\Delta_{SP}+p_1+1) - \left(\frac{(\beta_{SP}-\delta_{SP})\rho_D + (\beta_{SR}-\delta_{SR})\phi_1}{\bar{\rho}_S}\right)^{\Delta_{SP}+p_1}\right)}{p_1! (\beta_{SR} - \delta_{SR})^{\Delta_{SR}-p_1} (\Delta_{SP}+p_1) ((\beta_{SP} - \delta_{SP}) \rho_D + (\beta_{SR} - \delta_{SR}) \phi_1)^{\Delta_{SP}+p_1}}\right) \times \left(\frac{\left(\frac{\rho_D}{\Lambda_{RP}\bar{\rho}_R}\right)^{m_{RP}} \left(1 - \frac{(\bar{\phi}_1/\bar{\rho}_R \Lambda_1)^{N_1 m_1}}{\Gamma(N_1 m_1 + 1)}\right)}{\Gamma(m_{RP}+1)} + \sum_{p_2=0}^{N_1 m_1 - 1} \frac{(\Lambda_1 \rho_D)^{m_{RP}} (\bar{\phi}_1 \Lambda_{RP})^{p_2} \left(\Gamma(m_{RP}+p_2+1) - \left(\frac{\bar{\phi}_1 \Lambda_{RP} + \Lambda_1 \rho_D}{\Lambda_1 \bar{\rho}_R \Lambda_{RP}}\right)^{m_{RP}+p_2}\right)}{p_2! \Gamma(m_{RP}) (m_{RP}+p_2) \left(\bar{\phi}_1 \Lambda_{RP} + \Lambda_1 \rho_D\right)^{m_{RP}+p_2}}\right) \quad (33)$$

$$B_1^{\infty} = \widetilde{\sum} (m_{SR}, m_{SP}) \frac{(\beta_{SP} - \delta_{SP})^{-\Delta_{SP}}}{(\beta_{SR} - \delta_{SR})^{\Delta_{SR}} \Delta_{SP} \Delta_{SR}} \left(\frac{\rho_D (\beta_{SP} - \delta_{SP})}{\bar{\rho}_S}\right)^{\Delta_{SP}} \left(\Gamma(\Delta_{SR}+1) - \left(\frac{(\beta_{SR} - \delta_{SR}) \varphi_2}{\bar{\rho}_S}\right)^{\Delta_{SR}}\right) + \widetilde{\sum} (m_{SR}, m_{SP}) \sum_{p_3=0}^{\Delta_{SR}-1} \frac{\Gamma(\Delta_{SR}) \varphi_2^{p_3} \rho_D^{\Delta_{SP}} \left(\Gamma(\Delta_{SP}+p_3+1) - \left(\frac{(\beta_{SP}-\delta_{SP})\rho_D + (\beta_{SR}-\delta_{SR})\varphi_2}{\bar{\rho}_S}\right)^{\Delta_{SP}+p_3}\right)}{p_3! (\beta_{SR} - \delta_{SR})^{\Delta_{SR}-p_3} (\Delta_{SP}+p_3) ((\beta_{SP} - \delta_{SP}) \rho_D + (\beta_{SR} - \delta_{SR}) \varphi_2)^{\Delta_{SP}+p_3}} \quad (35)$$

$$B_2^{\infty} = \left(\frac{\rho_D}{\Lambda_{RP}\bar{\rho}_R}\right)^{m_{RP}} \frac{\left(1 - \frac{(\bar{\varphi}_2/\bar{\rho}_R \Lambda_2)^{N_1 m_1}}{\Gamma(N_2 m_2 + 1)}\right)}{\Gamma(m_{RP}+1)} + \sum_{p_3=0}^{N_2 m_2 - 1} \frac{(\Lambda_2 \rho_D)^{m_{RP}} (\bar{\varphi}_2 \Lambda_{RP})^{p_3}}{p_3! \Gamma(m_{RP}) (m_{RP}+p_3) (\bar{\varphi}_2 \Lambda_{RP} + \Lambda_2 \rho_D)^{m_{RP}+p_3}} \times \left(\Gamma(m_{RP}+p_3+1) - \left(\frac{\bar{\varphi}_2 \Lambda_{RP} + \Lambda_2 \rho_D}{\Lambda_2 \bar{\rho}_R \Lambda_{RP}}\right)^{m_{RP}+p_3}\right), \quad (36)$$

$$B_3^{\infty} = \left(\frac{\rho_D}{\Lambda_{RP}\bar{\rho}_R}\right)^{m_{RP}} \frac{\left(1 - \frac{(\bar{\varphi}_2/\bar{\rho}_R \Lambda_1)^{N_1 m_1}}{\Gamma(N_1 m_1 + 1)}\right)}{\Gamma(m_{RP}+1)} + \sum_{p_4=0}^{N_1 m_1 - 1} \frac{(\Lambda_1 \rho_D)^{m_{RP}} (\bar{\varphi}_2 \Lambda_{RP})^{p_4}}{p_4! \Gamma(m_{RP}) (m_{RP}+p_4) (\bar{\varphi}_2 \Lambda_{RP} + \Lambda_1 \rho_D)^{m_{RP}+p_4}} \times \left(\Gamma(m_{RP}+p_4+1) - \Gamma\left(\frac{\bar{\varphi}_2 \Lambda_{RP} + \Lambda_1 \rho_D}{\Lambda_1 \bar{\rho}_R \Lambda_{RP}}\right)^{m_{RP}+p_4}\right). \quad (37)$$

$$IP_{D_1}^{out} = \left(\widetilde{\sum} (m_{SR}, m_{SP}) \frac{(\beta_{SP} - \delta_{SP})^{-\Lambda_{SP}}}{(\beta_{SR} - \delta_{SR})^{\Lambda_{SR}}} \gamma\left(\Lambda_{SP}, \frac{\rho_D (\beta_{SP} - \delta_{SP})}{\bar{\rho}_S}\right) \Gamma\left(\Lambda_{SR}, \frac{(\beta_{SR} - \delta_{SR}) \eta}{\bar{\rho}_S}\right) + \widetilde{\sum} (m_{SR}, m_{SP}) \sum_{p=0}^{\Lambda_{SR}-1} \frac{\Gamma(\Lambda_{SR}) \eta^p \rho_D^{\Lambda_{SP}} \Gamma\left(\Lambda_{SP}+p, \frac{(\beta_{SP}-\delta_{SP})\rho_D + (\beta_{SR}-\delta_{SR})\eta}{\bar{\rho}_S}\right)}{p! (\beta_{SR} - \delta_{SR})^{\Lambda_{SR}-p} ((\beta_{SP} - \delta_{SP}) \rho_D + (\beta_{SR} - \delta_{SR}) \eta)^{\Lambda_{SP}+p}}\right) \times \left(\frac{\gamma\left(m_{RP}, \frac{\rho_D}{\Lambda_{RP}\bar{\rho}_R}\right) \Gamma\left(N_E m_E, \frac{\bar{\phi}_3}{\bar{\rho}_R \Lambda_E}\right)}{\Gamma(m_{RP}) \Gamma(N_E m_E)} + \sum_{p=0}^{N_E m_E - 1} \frac{(\Lambda_E \rho_D)^{m_{RP}} \left(\bar{\phi}_3 \Lambda_{RP}\right)^p \Gamma\left(m_{RP}+p, \frac{\bar{\phi}_3 \Lambda_{RP} + \Lambda_E \rho_D}{\Lambda_E \bar{\rho}_R \Lambda_{RP}}\right)}{p! \Gamma(m_{RP}) \left(\bar{\phi}_3 \Lambda_{RP} + \Lambda_E \rho_D\right)^{m_{RP}+p}}\right) \quad (39)$$

where $\eta = \max(\phi_1, \phi_2)$ and $\bar{\phi}_3 = \frac{\gamma_{E_1}}{(b_1 - \gamma_{E_1} k_E^2)}$. After some variable substitutions and manipulations C_1 is expressed as

$$\begin{aligned} C_1 &= \int_0^{\frac{\rho_D}{\bar{\rho}_S}} f_{\mathcal{H}_{SP}}(x) \int_{\frac{\eta}{\bar{\rho}_S}}^{\infty} f_{\mathcal{H}_{SR}}(y) dy dx \\ &= \widetilde{\sum} (m_{SR}, m_{SP}) \frac{(\beta_{SP} - \delta_{SP})^{-\Lambda_{SP}}}{(\beta_{SR} - \delta_{SR})^{\Lambda_{SR}}} \\ &\quad \times \gamma\left(\Lambda_{SP}, \frac{\rho_D (\beta_{SP} - \delta_{SP})}{\bar{\rho}_S}\right) \Gamma\left(\Lambda_{SR}, \frac{(\beta_{SR} - \delta_{SR})\eta}{\bar{\rho}_S}\right). \end{aligned} \tag{41}$$

Next, C_2 can be further calculated as follow

$$\begin{aligned} C_2 &= \int_{\frac{\rho_D}{\bar{\rho}_S}}^{\infty} f_{\mathcal{H}_{SP}}(x) \int_{\frac{\eta x}{\rho_D}}^{\infty} f_{\mathcal{H}_{SR}}(y) dy dx \\ &= \widetilde{\sum} (m_{SR}, m_{SP}) \sum_{p=0}^{\Lambda_{SR}-1} \frac{\Gamma(\Lambda_{SR}) \eta^p \rho_D^{\Lambda_{SP}}}{p! (\beta_{SR} - \delta_{SR})^{\Lambda_{SR}-p}} \\ &\quad \times \frac{\Gamma\left(\Lambda_{SP} + p, \frac{(\beta_{SP} - \delta_{SP})\rho_D + (\beta_{SR} - \delta_{SR})\eta}{\bar{\rho}_S}\right)}{((\beta_{SP} - \delta_{SP})\rho_D + (\beta_{SR} - \delta_{SR})\eta)^{\Lambda_{SP}+p}}. \end{aligned} \tag{42}$$

Similarly, C_3 is expressed as

$$\begin{aligned} C_3 &= \int_0^{\frac{\rho_D}{\bar{\rho}_R}} f_{|h_{RP}|^2}(x) \int_{\frac{\bar{\varphi}_3}{\bar{\rho}_R}}^{\infty} f_{\mathcal{H}_E}(y) dy dx \\ &= \frac{\gamma\left(m_{RP}, \frac{\rho_D}{\Lambda_{RP} \bar{\rho}_R}\right) \Gamma\left(N_E m_E, \frac{\bar{\phi}_3}{\bar{\rho}_R \Lambda_E}\right)}{\Gamma(m_{RP}) \Gamma(N_E m_E)}. \end{aligned} \tag{43}$$

Furthermore, C_4 can be easily calculated by

$$\begin{aligned} C_4 &= \int_{\frac{\rho_D}{\bar{\rho}_R}}^{\infty} f_{|h_{RP}|^2}(x) \int_{\frac{\bar{\phi}_{3x}}{\rho_D}}^{\infty} f_{\mathcal{H}_E}(y) dy dx \\ &= \sum_{p=0}^{N_E m_E - 1} \frac{(\Lambda_E \rho_D)^{m_{RP}} \left(\bar{\phi}_3 \Lambda_{RP}\right)^p}{p! \Gamma(m_{RP}) (\bar{\varphi}_3 \Lambda_{RP} + \Lambda_E \rho_D)^{m_{RP}+p}} \\ &\quad \times \Gamma\left(m_{RP} + p, \frac{\bar{\phi}_3 \Lambda_{RP} + \Lambda_E \rho_D}{\Lambda_E \bar{\rho}_R \Lambda_{RP}}\right) \end{aligned} \tag{44}$$

Finally, our expected result can be achieved by combining (41), (42), (43) and (44).

The proof is completed.

E. INTERCEPT PROBABILITY OF D_2

The intercept probability of D_2 is given as [37]

$$IP_{D_2}^{out} = \Pr\left(\gamma_{R,x_1} > \gamma_{th_1}, \gamma_{R,x_2} > \gamma_{th_2}, \gamma_{E,x_2} > \gamma_{E_2}\right) \tag{45}$$

According to the above explanations, with $\bar{\phi}_4 = \frac{\gamma_{E_2}}{(b_2 - b_1 \gamma_{E_2} - k_E^2 \gamma_{E_2})}$ the closed-form expression of user D_2, i.e. $IP_{D_2}^{out}$ is obtained as (46), as shown at the bottom of the page.

F. THROUGHPUT PERFORMANCE

It can be further evaluated other metric, i.e. the overall throughput can be achieved based on obtained outage probabilities. In delay-limited mode, at fixed target rates R_1, R_2 the throughput can be achieved. As a result, the overall throughput can be formulated as [38]

$$\mathcal{T}_{total} = \left(1 - P_{D_1}^{out}\right) R_1 + \left(1 - P_{D_2}^{out}\right) R_2. \tag{47}$$

IV. NUMERICAL RESULTS

In this section, to verify mathematical analysis, it is necessary to simulate and illustrate for proposed assisted CR-NOMA scheme. Here, the shadowing scenarios of the satellite links $\mathcal{H}_j$, including the heavy shadowing (HS) with $b_j, m_j, \Omega_j = (1, 0.063, 0.0007)$ and average shadowing (AS) with $b_j, m_j, \Omega_j = (5, 0.251, 0.279)$ as [39].

Next, we set power allocation factors $a_1 = b_1 = 0.2$, $a_2 = b_2 = 0.8$, $\bar{\rho} = \bar{\rho}_S = \bar{\rho}_R$, $k = k_{RD_i} = k_{SR} = k_E$, $N = N_1 = N_2 = N_E$, the target rates $R_1 = R_2 = 0.5$ bit per channel use (BPCU) except for specific cases, the channel gains $\lambda_1 = 1$, $\lambda_2 = 2$, λ_{RP} and $m = m_1 = m_2 = m_{RP} = m_E$. Moreover, case of $m = 1$ is equivalent with the Rayleigh fading channel model. In these following figures, Monte-Carlo simulations are performed to validate the analytical results.

Fig. 2 shows the comparison of OP performance with HS and AS schemes for two users. By increasing average SNR at the source, OP decreases significantly, especially in high region of SNR, i.e. $\bar{\rho}$. As can be observed, analytical results agree well with the Monte Carlo simulations, which

$$\begin{aligned} IP_{D_2}^{out} &= \left(\widetilde{\sum} (m_{SR}, m_{SP}) \frac{(\beta_{SP} - \delta_{SP})^{-\Lambda_{SP}}}{(\beta_{SR} - \delta_{SR})^{\Lambda_{SR}}} \gamma\left(\Lambda_{SP}, \frac{\rho_D (\beta_{SP} - \delta_{SP})}{\bar{\rho}_S}\right) \Gamma\left(\Lambda_{SR}, \frac{(\beta_{SR} - \delta_{SR})\eta}{\bar{\rho}_S}\right)\right. \\ &\quad \left. + \widetilde{\sum} (m_{SR}, m_{SP}) \sum_{p=0}^{\Lambda_{SR}-1} \frac{\Gamma(\Lambda_{SR}) \eta^p \rho_D^{\Lambda_{SP}} \Gamma\left(\Lambda_{SP} + p, \frac{(\beta_{SP} - \delta_{SP})\rho_D + (\beta_{SR} - \delta_{SR})\eta}{\bar{\rho}_S}\right)}{p! (\beta_{SR} - \delta_{SR})^{\Lambda_{SR}-p} ((\beta_{SP} - \delta_{SP})\rho_D + (\beta_{SR} - \delta_{SR})\eta)^{\Lambda_{SP}+p}}\right) \\ &\quad \times \left(\frac{\gamma\left(m_{RP}, \frac{\rho_D}{\Lambda_{RP} \bar{\rho}_R}\right) \Gamma\left(N_E m_E, \frac{\bar{\phi}_4}{\bar{\rho}_R \Lambda_E}\right)}{\Gamma(m_{RP}) \Gamma(N_E m_E)} + \sum_{p=0}^{N_E m_E - 1} \frac{(\Lambda_E \rho_D)^{m_{RP}} \left(\bar{\phi}_4 \Lambda_{RP}\right)^p}{p! \Gamma(m_{RP}) \left(\bar{\phi}_4 \Lambda_{RP} + \Lambda_E \rho_D\right)^{m_{RP}+p}} \Gamma\left(m_{RP} + p, \frac{\bar{\phi}_4 \Lambda_{RP} + \Lambda_E \rho_D}{\Lambda_E \bar{\rho}_R \Lambda_{RP}}\right)\right) \end{aligned} \tag{46}$$

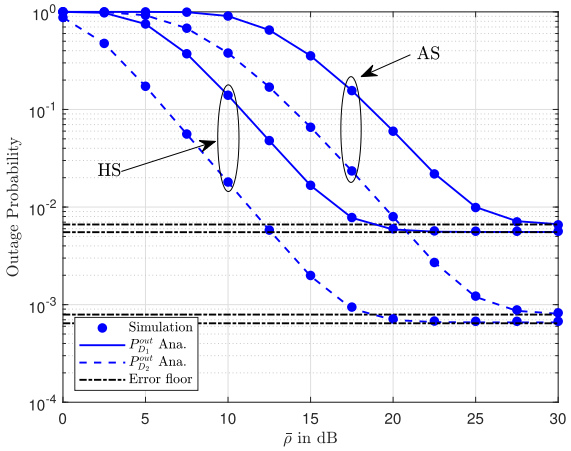

FIGURE 2. The outage probability versus $\bar{\rho}$, where $M = N = m = 2$, $\rho_D = 20$dB and $k = 0.1$.

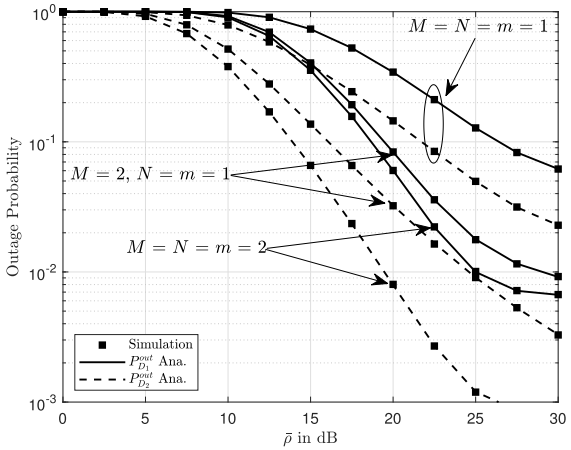

FIGURE 3. The outage probability versus $\bar{\rho}$, with different values of M, N, m, where $\rho_D = 20$dB, $k = 0.1$ and the satellite link is set HS case.

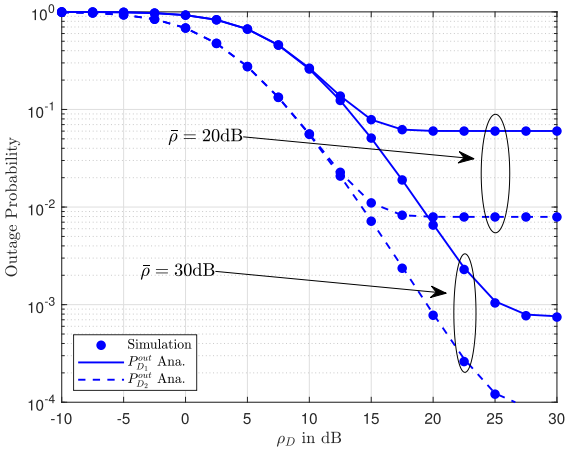

FIGURE 4. The outage probability versus ρ_D, with different values of ρ, where $M = N = m = 2$, $k = 0.1$ and the satellite link is set HS case.

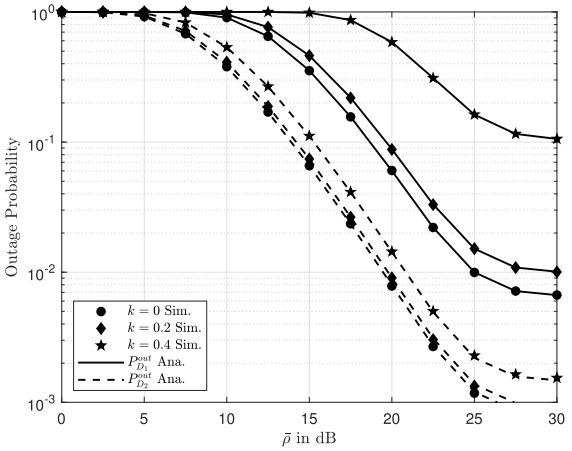

FIGURE 5. The outage probability versus $\bar{\rho}$, with different values of k, where $M = N = m = 2$, $\rho_D = 20$dB, and the satellite link is set HS case.

confirm the corrections of derived expressions. Moreover, an increasing of $\bar{\rho}$ obviously improves the SINR, then the corresponding OP performance of two users can be improved. However, such OP depends on target rates, then these curves become saturated. It is worth noting that when adjusting the power allocation coefficient reasonably, we can reduce OP performance gap among two users. The reason is that the OP depends on SINR, while SINR contain power allocation factors. This phenomenon implies that a reliable transmission can be achieved by introducing the higher SNR at source and reasonable selection of power allocation factors.

Fig. 3 demonstrates the OP performance of the considered NOMA-HSTCN for different antenna configurations, where the satellite-relay link undergoes HS case. As expected, the OP improves with an increase in the number of antennas, demonstrating the advantages of employing multiple antennas and beamforming in such systems. For example, the antenna configuration with $M = N = 2$ can achieve a significant enhancement compared with systems with case of $M = N = 1$. Similarly, the power constraint with primary network contributes to vary OP of two users as shown in Fig. 4. In this observation, $\bar{\rho} = 30$ is reported as better OP for two users under evaluation trends of OP by adjusting ρ_D from -10 to 30 dB.

Under impact of hardware imperfection, OP changes once we vary value of k, shown in Fig. 5. It can be concluded that user D_2 has little impact by hardware imperfection. In contrast, there are gaps among three cases of $k = 0, 0.2, 0.4$ as considering OP performance of user D_1. The reason is that SINRs depend on k.

The impacts of power allocation factors a_1, b_1 on OP performance can be seen clearly as Fig. 6. As seen from (9), (10), and (11), OP can be decided by varying SINRs while such SINRs depend on power allocation factors. The opposite trends of OP for two users once we increase a_1, b_1 from 0 to 0.5. Of course, systems relying on OMA do not depend on such power factors, it is indicated as straight lines regardless of varying of a_1, b_1.

In Fig. 7, we can see trends of the IP for two users under various configurations of satellite link modes (AS and HS) as well as antennas. It can be confirmed that user D_2 more secure compared with D_1 regardless of other set of satellite links or the number of antennas, which means that the superiority of user D_2 compared with user D_1 in term of OP and IP are same. In addition, in Fig. 8 there are similar

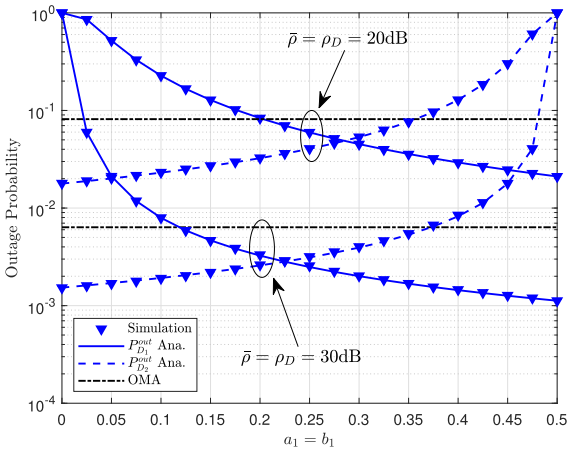

FIGURE 6. The outage probability versus $a_1 = b_1$, with different values of $\bar{\rho} = \rho_D$, where $M = N = m = 2$, $k = 0.1$ and the satellite link is set HS case.

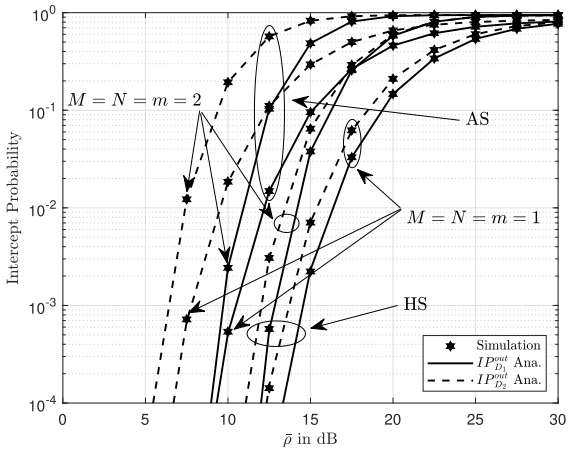

FIGURE 7. The Intercept Probability versus ρ, with different values of M, N, m and channel parameter of satellite link, where $\rho_D = 20$dB, $k = 0.1$, $\lambda_E = 0.1$, $\gamma_{E_1} = \gamma_{E_2} = 1$ and $R_1 = R_2 = 1$.

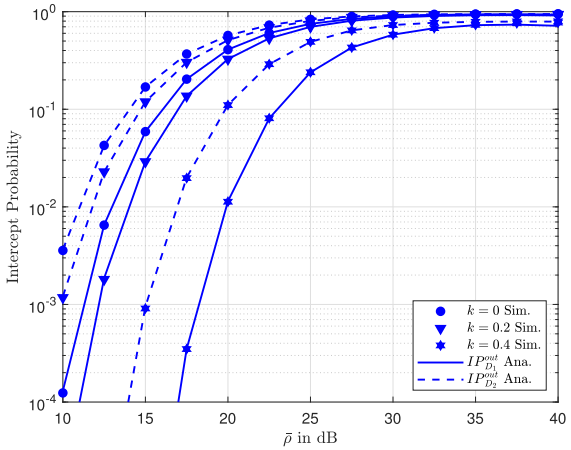

FIGURE 8. The Intercept Probability versus ρ, with different values of k, where $M = N = m = 2$, $\rho_D = 20$dB, $\lambda_E = 0.1$, $\gamma_{E_1} = \gamma_{E_2} = 1$, $R_1 = R_2 = 0.5$ and the satellite link is set HS case.

performance gap regarding IP of two users when we vary value of k which is reported impact of hardware noise to IP performance. Of course, ideal hardware exhibits the best IP performance. Therefore, it can help when designing NOMA-HSTCN communication systems to combat undesired effects related hardware.

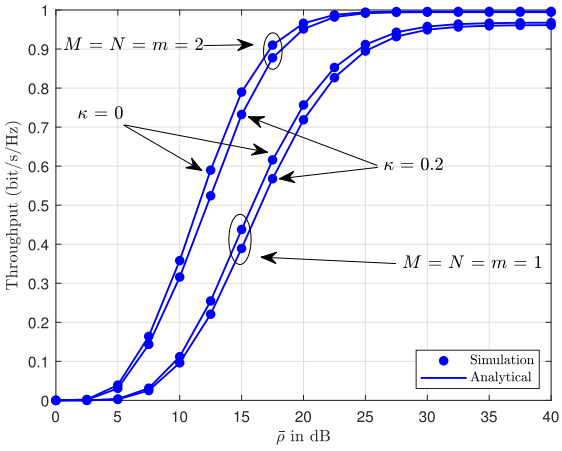

FIGURE 9. Throughput of system with $\rho_D = 20$dB, $R_1 = R_2 = 0.5$ and the satellite link is set HS case.

In Fig. 9, we can see how transmit SNR at source contributes to change of the throughput for two users under various configurations of satellite links as well as the number of antennas. It can be reported from (20) and (24) to confirm that the trend of throughput for two users can be predicted, i.e. it is very high at high SNR region.

V. CONCLUSION

In this paper, we have investigated the effects of hardware impairments on the reliability and security for NOMA-HSTCN systems by enabling multiple antennas design. The practical factor of hardware impairments are studied insight fully. Specifically, we derive the closed-form analytical expressions of the OP and IP to highlight as important performance metrics, and analyze the limitation of OP in the high SNR region. The results obtained have been verified by Monte Carlo simulation. These results show that as the level of hardware impairment increases, the user's OP reduce significantly, and the IP decreases as well. The different trends of curves in term of OP is caused by the power allocation parameters. It can be concluded that the severity of the performance degradation depends on several factors, including the power allocation ratio, the transmit SNR at the source, and the quality of channels. We can extend to generic framework to analyse performance of larger number of NOMA users in future work.

APPENDIX A

With the help (4) and (5), the term A_1 can be written as

$$\begin{aligned} A_1 &= \Pr\left(\frac{P_S a_1 \mathcal{H}_{SR}}{P_S k_{SR}^2 \mathcal{H}_{SR} + \sigma_R^2} > \gamma_{th_1}\right) \\ &= \Pr\left(\bar{\rho}_S < \frac{\rho_D}{\mathcal{H}_{SP}}, \frac{\bar{\rho}_S a_1 \mathcal{H}_{SR}}{\bar{\rho}_S k_{SR}^2 \mathcal{H}_{SR} + 1} > \gamma_{th_1}\right) \\ &\quad + \Pr\left(\bar{\rho}_S > \frac{\rho_D}{\mathcal{H}_{SP}}, \frac{\rho_D a_1 \mathcal{H}_{SR}}{\rho_D k_{SR}^2 \mathcal{H}_{SR} + \mathcal{H}_{SP}} > \gamma_{th_1}\right), \quad (48) \end{aligned}$$

where $\sigma^2 = \sigma_R^2 = \sigma_i^2 = \sigma_E^2$, $\bar{\rho}_S = \frac{\bar{P}_S}{\sigma^2}$ and $\rho_D = \frac{\bar{P}_P}{\sigma^2}$. First, we denote the first term of (48) is A_{1_1} and it can be computed by

$$A_{1\_1} = \Pr\left(\mathcal{H}_{SP} < \frac{\rho_D}{\bar{\rho}_S}, \mathcal{H}_{SR} > \frac{\phi_1}{\bar{\rho}_S}\right) = \int_0^{\frac{\rho_D}{\bar{\rho}_S}} f_{\mathcal{H}_{SP}}(x) \int_{\frac{\phi_1}{\bar{\rho}_S}}^{\infty} f_{\mathcal{H}_{SR}}(y) dy dx, \quad (49)$$

where $\phi_1 = \frac{\gamma_{th_1}}{(a_1 - k_{SR}^2 \gamma_{th_1})}$.

Moreover, substituting (16) into (49) we can be calculate A_{1_1} as

$$A_{1\_1} = \widetilde{\sum}(m_{SR}, m_{SP}) \int_0^{\frac{\rho_D}{\bar{\rho}_S}} x^{\Delta_{SP}-1} e^{-(\beta_{SP}-\delta_{SP})x} \times \int_{\frac{\phi_1}{\bar{\rho}_S}}^{\infty} y^{\Delta_{SR}-1} e^{-(\beta_{SR}-\delta_{SR})y} dx dy, \quad (50)$$

where

$$\widetilde{\sum}(m_{SR}, m_{SP}) = \sum_{i_1=0}^{m_{SR}-1} \cdots \sum_{i_M=0}^{m_{SR}-1} \Theta(SR, M) \times \sum_{i_1=0}^{m_{SP}-1} \cdots \sum_{i_M=0}^{m_{SP}-1} \Theta(SP, M). \quad (51)$$

Based on [45, Eq. 3.351.1, Eq. 3.351.2], A_{1_1} is obtained as

$$A_{1\_1} = \widetilde{\sum}(m_{SR}, m_{SP}) \frac{(\beta_{SP}-\delta_{SP})^{-\Delta_{SP}}}{(\beta_{SR}-\delta_{SR})^{\Delta_{SR}}} \times \gamma\left(\Delta_{SP}, \frac{\rho_D(\beta_{SP}-\delta_{SP})}{\bar{\rho}_S}\right) \Gamma\left(\Delta_{SR}, \frac{\phi_1(\beta_{SR}-\delta_{SR})}{\bar{\rho}_S}\right). \quad (52)$$

Second, the second term of (48) is A_{1_2} and it can be expressed as

$$A_{1\_2} = \Pr\left(\mathcal{H}_{SP} > \frac{\rho_D}{\bar{\rho}_S}, \mathcal{H}_{SR} > \frac{\phi_1 \mathcal{H}_{SP}}{\rho_D}\right) = \int_{\frac{\rho_D}{\bar{\rho}_S}}^{\infty} f_{\mathcal{H}_{SP}}(x) \int_{\frac{\phi_1 x}{\rho_D}}^{\infty} f_{\mathcal{H}_{SR}}(y) dy dx. \quad (53)$$

Furthermore, it can be calculated as

$$A_{1\_2} = \widetilde{\sum}(m_{SR}, m_{SP}) \int_{\frac{\rho_D}{\bar{\rho}_S}}^{\infty} x^{\Delta_{SP}-1} e^{-(\beta_{SP}-\delta_{SP})x} \times \int_{\frac{\phi_1 x}{\rho_D}}^{\infty} y^{\Delta_{SR}-1} e^{-(\beta_{SR}-\delta_{SR})y} dy dx. \quad (54)$$

After some algebraic manipulations, A_{1_2} can be obtain as

$$A_{1\_2} = \widetilde{\sum}(m_{SR}, m_{SP}) \sum_{p_1=0}^{\Delta_{SR}-1} \frac{\Gamma(\Delta_{SR}) \phi_1^{p_1} \rho_D^{\Delta_{SP}}}{p_1! (\beta_{SR}-\delta_{SR})^{\Delta_{SR}-p_1}} \times \frac{\Gamma\left(\Delta_{SP}+p_1, \frac{(\beta_{SP}-\delta_{SP})\rho_D + (\beta_{SR}-\delta_{SR})\phi_1}{\bar{\rho}_S}\right)}{((\beta_{SP}-\delta_{SP})\rho_D + (\beta_{SR}-\delta_{SR})\phi_1)^{\Delta_{SP}+p_1}} \quad (55)$$

Finally, by substituting (52) and (55) into (48) we obtain (20) and the proof is completed.

APPENDIX B

By substituting (5) and (11) into (19), A_2 is rewritten as

$$A_2 = \Pr\left(\frac{P_R b_1 \mathcal{H}_{RD_1}}{P_R k_{RD_1}^2 \mathcal{H}_{RD_1} + \sigma_1^2} > \gamma_{th_1}\right) = \Pr\left(\bar{\rho}_R < \frac{\rho_D}{|h_{RP}|^2}, \frac{\bar{\rho}_R b_1 \mathcal{H}_{RD_1}}{\bar{\rho}_R k_{RD_1}^2 \mathcal{H}_{RD_1} + 1} > \gamma_{th_1}\right) + \Pr\left(\bar{\rho}_R > \frac{\rho_D}{|h_{RP}|^2}, \frac{\rho_D b_1 \mathcal{H}_{RD_1}}{\rho_D k_{RD_1}^2 \mathcal{H}_{RD_1} + |h_{RP}|^2} > \gamma_{th_1}\right) \quad (56)$$

Similarly, we denote the first and second term of (56) are A_{2_1} and A_{2_2} respectively. Then, A_{2_1} is express as

$$A_{2\_1} = \Pr\left(|h_{RP}|^2 < \frac{\rho_D}{\bar{\rho}_R}, \mathcal{H}_{RD_1} > \frac{\bar{\phi}_1}{\bar{\rho}_R}\right) = \int_0^{\frac{\rho_D}{\bar{\rho}_R}} f_{|h_{RP}|^2}(x) \int_{\frac{\bar{\phi}_1}{\bar{\rho}_R}}^{\infty} f_{\mathcal{H}_{RD_1}}(y) dy dx \quad (57)$$

where $\bar{\phi}_1 = \frac{\gamma_{th_1}}{\left(b_1 - \gamma_{th_1} k_{RD_1}^2\right)}$. With the help of (17), (18) and after some variable substitutions and manipulations, we can obtain A_{2_1} as

$$A_{2\_1} = \int_0^{\frac{\rho_D}{\bar{\rho}_R}} \frac{x^{m_{RP}-1}}{\Gamma(m_{RP}) \Lambda_{RP}^{m_{RP}}} e^{-\frac{x}{\Lambda_{RP}}} \times \int_{\frac{\bar{\phi}_1}{\bar{\rho}_R}}^{\infty} \frac{y^{N_1 m_1 - 1}}{\Gamma(N_1 m_1) \Lambda_1^{N_1 m_1}} e^{-\frac{y}{\Lambda_1}} dy dx = \frac{\gamma\left(m_{RP}, \frac{\rho_D}{\Lambda_{RP}\bar{\rho}_R}\right) \Gamma\left(N_1 m_1, \frac{\bar{\phi}_1}{\bar{\rho}_R \Lambda_v}\right)}{\Gamma(m_{RP}) \Gamma(N_1 m_1)}. \quad (58)$$

Furthermore, the term A_{2_2} is expressed as

$$A_{2\_2} = \Pr\left(|h_{RP}|^2 > \frac{\rho_D}{\bar{\rho}_R}, \mathcal{H}_{RD_1} > \frac{\bar{\phi}_1 |h_{RP}|^2}{\rho_D}\right) = \int_0^{\infty} f_{|h_{RP}|^2}(x) \int_{\frac{\bar{\phi}_1 x}{\rho_D}}^{\infty} f_{\mathcal{H}_{RD_1}}(y) dy dx \quad (59)$$

Similar in (55), A_{2_2} is given by

$$A_{2\_2} = \sum_{p_2=0}^{N_1 m_1 - 1} \frac{(\Lambda_1 \rho_D)^{m_{RP}} \left(\bar{\phi}_1 \Lambda_{RP}\right)^{p_2}}{p_2! \Gamma(m_{RP}) \left(\bar{\phi}_1 \Lambda_{RP} + \Lambda_1 \rho_D\right)^{m_{RP}+p_2}} \times \Gamma\left(m_{RP} + p_2, \frac{\bar{\phi}_1 \Lambda_{RP} + \Lambda_1 \rho_D}{\Lambda_1 \bar{\rho}_R \Lambda_{RP}}\right). \quad (60)$$

Now, using (58) and (60), the expected result can be attained.

This completes the proof.

REFERENCES

[1] X. Zhang, D. Guo, K. An, Z. Chen, B. Zhao, Y. Ni, and B. Zhang, "Performance analysis of NOMA-based cooperative spectrum sharing in hybrid satellite-terrestrial networks," *IEEE Access*, vol. 7, pp. 172321–172329, 2019.

[2] Z. Li, F. Xiao, S. Wang, T. Pei, and J. Li, "Achievable rate maximization for cognitive hybrid satellite-terrestrial networks with AF-relays," *IEEE J. Sel. Areas Commun.*, vol. 36, no. 2, pp. 304–313, Feb. 2018.

[3] L. Yang and M. O. Hasna, "Performance analysis of amplify- and-forward hybrid satellite-terrestrial networks with cochannel interference," *IEEE Trans. Commun.*, vol. 63, no. 12, pp. 5052–5061, Dec. 2015.

[4] P. K. Upadhyay and P. K. Sharma, "Max-max user-relay selection scheme in multiuser and multirelay hybrid satellite-terrestrial relay systems," *IEEE Commun. Lett.*, vol. 20, no. 2, pp. 268–271, Feb. 2016.

[5] M. K. Arti, "Channel estimation and detection in hybrid satellite–terrestrial communication systems," *IEEE Trans. Veh. Technol.*, vol. 65, no. 7, pp. 5764–5771, Jul. 2016.

[6] K. An, M. Lin, and T. Liang, "On the performance of multiuser hybrid satellite-terrestrial relay networks with opportunistic scheduling," *IEEE Commun. Lett.*, vol. 19, no. 10, pp. 1722–1725, Oct. 2015.

[7] V. Singh, S. Solanki, and P. K. Upadhyay, "Cognitive relaying cooperation in satellite-terrestrial systems with multiuser diversity," *IEEE Access*, vol. 6, pp. 65539–65547, Oct. 2018.

[8] X. Zhang, B. Zhang, K. An, Z. Chen, S. Xie, H. Wang, L. Wang, and D. Guo, "Outage performance of NOMA-based cognitive hybrid satellite-terrestrial overlay networks by amplify- and-forward protocols," *IEEE Access*, vol. 7, pp. 85372–85381, 2019.

[9] X. Zhu, C. Jiang, L. Kuang, N. Ge, S. Guo, and J. Lu, "Cooperative transmission in integrated terrestrial-satellite networks," *IEEE Netw.*, vol. 33, no. 3, pp. 204–210, May 2019.

[10] W. Liang, S. X. Ng, and L. Hanzo, "Cooperative overlay spectrum access in cognitive radio networks," *IEEE Commun. Surveys Tuts.*, vol. 19, no. 3, pp. 1924–1944, 3rd Quart., 2017.

[11] F. Li, K.-Y. Lam, N. Zhao, X. Liu, K. Zhao, and L. Wang, "Spectrum trading for satellite communication systems with dynamic bargaining," *IEEE Trans. Commun.*, vol. 66, no. 10, pp. 4680–4693, Oct. 2018.

[12] K. An, M. Lin, W.-P. Zhu, Y. Huang, and G. Zheng, "Outage performance of cognitive hybrid satellite–terrestrial networks with interference constraint," *IEEE Trans. Veh. Technol.*, vol. 65, no. 11, pp. 9397–9404, Nov. 2016.

[13] Z. Chen, D. Guo, G. Ding, X. Tong, H. Wang, and X. Zhang, "Optimized power control scheme for global throughput of cognitive satellite-terrestrial networks based on non-cooperative game," *IEEE Access*, vol. 7, pp. 81652–81663, 2019.

[14] Z. Lin, M. Lin, W.-P. Zhu, J.-B. Wang, and J. Cheng, "Robust secure beamforming for wireless powered cognitive satellite-terrestrial networks," *IEEE Trans. Cognit. Commun. Netw.*, early access, Aug. 12, 2020, doi: 10.1109/TCCN.2020.3016096.

[15] P. K. Sharma, P. K. Upadhyay, D. B. D. Costa, P. S. Bithas, and A. G. Kanatas, "Performance analysis of overlay spectrum sharing in hybrid satellite-terrestrial systems with secondary network selection," *IEEE Trans. Wireless Commun.*, vol. 16, no. 10, pp. 6586–6601, Oct. 2017.

[16] D.-T. Do, M.-S.-V. Nguyen, F. Jameel, R. Jantti, and I. S. Ansari, "Performance evaluation of relay-aided CR-NOMA for beyond 5G communications," *IEEE Access*, vol. 8, pp. 134838–134855, 2020.

[17] X. Li, Q. Wang, Y. Liu, T. A. Tsiftsis, Z. Ding, and A. Nallanathan, "UAV-aided multi-way NOMA networks with residual hardware impairments," *IEEE Wireless Commun. Lett.*, vol. 9, no. 9, pp. 1538–1542, Sep. 2020.

[18] D.-T. Do, A.-T. Le, and B. M. Lee, "NOMA in cooperative underlay cognitive radio networks under imperfect SIC," *IEEE Access*, vol. 8, pp. 86180–86195, 2020.

[19] D.-T. Do and A.-T. Le, "NOMA based cognitive relaying: Transceiver hardware impairments, relay selection policies and outage performance comparison," *Comput. Commun.*, vol. 146, pp. 144–154, Oct. 2019.

[20] T.-L. Nguyen and D.-T. Do, "Power allocation schemes for wireless powered NOMA systems with imperfect CSI: An application in multiple antenna-based relay," *Int. J. Commun. Syst.*, vol. 31, no. 15, p. e3789, Oct. 2018.

[21] D.-T. Do, "Time power switching based relaying protocol in energy harvesting mobile node: Optimal throughput analysis," *Mobile Inf. Syst.*, vol. 2015, pp. 1–8, Jun. 2015.

[22] T. N. Kieu, D. O. Dinh-Thuan, X. N. Xuan, T. N. Nhat, and H. H. Duy, "Wireless information and power transfer for full duplex relaying networks: Performance analysis," in *Recent Advances in Electrical Engineering and Related Sciences* (Lecture Notes in Electrical Engineering), vol. 371, V. Duy, T. Dao, I. Zelinka, H. S. Choi, and M. Chadli, Eds. Cham, Switzerland: Springer, 2015.

[23] S. Arzykulov, T. A. Tsiftsis, G. Nauryzbayev, and M. Abdallah, "Outage performance of cooperative underlay CR-NOMA with imperfect CSI," *IEEE Commun. Lett.*, vol. 23, no. 1, pp. 176–179, Jan. 2019.

[24] Z. Song, X. Wang, Y. Liu, and Z. Zhang, "Joint spectrum resource allocation in NOMA-based cognitive radio network with SWIPT," *IEEE Access*, vol. 7, pp. 89594–89603, 2019.

[25] J. Du, F. R. Yu, G. Lu, J. Wang, J. Jiang, and X. Chu, "MEC-assisted immersive VR video streaming over terahertz wireless networks: A deep reinforcement learning approach," *IEEE Internet Things J.*, vol. 7, no. 10, pp. 9517–9529, Oct. 2020.

[26] J. Du, L. Zhao, X. Chu, F. R. Yu, J. Feng, and C.-L. I, "Enabling low-latency applications in LTE—A based mixed fog/cloud computing systems," *IEEE Trans. Veh. Technol.*, vol. 68, no. 2, pp. 1757–1771, Feb. 2019.

[27] V. Singh, V. Bankey, and P. K. Upadhyay, "Underlay cognitive hybrid satellite-terrestrial networks with cooperative-NOMA," in *Proc. IEEE Wireless Commun. Netw. Conf. (WCNC)*, Seoul, South Korea, May 2020, pp. 1–6.

[28] V. Singh, P. K. Upadhyay, and M. Lin, "On the performance of NOMA-assisted overlay multiuser cognitive satellite-terrestrial networks," *IEEE Wireless Commun. Lett.*, vol. 9, no. 5, pp. 638–642, May 2020.

[29] M. Lin, Z. Lin, W.-P. Zhu, and J.-B. Wang, "Joint beamforming for secure communication in cognitive satellite terrestrial networks," *IEEE J. Sel. Areas Commun.*, vol. 36, no. 5, pp. 1017–1029, May 2018.

[30] W. Cao, Y. Zou, Z. Yang, and J. Zhu, "Relay selection for improving physical-layer security in hybrid satellite-terrestrial relay networks," *IEEE Access*, vol. 6, pp. 65275–65285, 2018.

[31] B. Li, Z. Fei, Z. Chu, F. Zhou, K.-K. Wong, and P. Xiao, "Robust chance-constrained secure transmission for cognitive satellite–terrestrial networks," *IEEE Trans. Veh. Technol.*, vol. 67, no. 5, pp. 4208–4219, May 2018.

[32] A. M. K. and M. R. Bhatnagar, "Beamforming and combining in hybrid satellite-terrestrial cooperative systems," *IEEE Commun. Lett.*, vol. 18, no. 3, pp. 483–486, Mar. 2014.

[33] K. An, J. Ouyang, M. Lin, and T. Liang, "Outage analysis of multi-antenna cognitive hybrid satellite-terrestrial relay networks with beamforming," *IEEE Commun. Lett.*, vol. 19, no. 7, pp. 1157–1160, Jul. 2015.

[34] H. Wu, Y. Zou, J. Zhu, X. Xue, and T. Tsiftsis, "Secrecy performance of hybrid satellite-terrestrial relay systems with hardware impairments," in *Proc. ICC-IEEE Int. Conf. Commun. (ICC)*, Shanghai, China, May 2019, pp. 1–6.

[35] M. K. Simon and M.-S. Alouini, *Digital Communications over Fading Channels: A Unified Approach to Performance Analysis*. Hoboken, NJ, USA: Wiley, 2000.

[36] D. B. D. Costa and S. Aissa, "Cooperative dual-hop relaying systems with beamforming over Nakagami-m fading channels," *IEEE Trans. Wireless Commun.*, vol. 8, no. 8, pp. 3950–3954, Aug. 2009.

[37] X. Li, M. Zhao, X.-C. Gao, L. Li, D.-T. Do, K. M. Rabie, and R. Kharel, "Physical layer security of cooperative NOMA for IoT networks under I/Q imbalance," *IEEE Access*, vol. 8, pp. 51189–51199, 2020.

[38] Y. Liu, Z. Ding, M. Elkashlan, and H. V. Poor, "Cooperative non-orthogonal multiple access with simultaneous wireless information and power transfer," *IEEE J. Sel. Areas Commun.*, vol. 34, no. 4, pp. 938–953, Apr. 2016.

[39] N. I. Miridakis, D. D. Vergados, and A. Michalas, "Dual-hop communication over a satellite relay and shadowed Rician channels," *IEEE Trans. Veh. Technol.*, vol. 64, no. 9, pp. 4031–4040, Sep. 2015.
[40] V. Bankey and P. K. Upadhyay, "Ergodic secrecy capacity analysis of multiuser hybrid satellite-terrestrial relay networks with multiple eavesdroppers," in *Proc. IEEE Int. Conf. Commun. Workshops (ICC Workshops)*, Shanghai, China, May 2019, pp. 1–6.
[41] V. Bankey, V. Singh, and P. K. Upadhyay, "Physical layer secrecy of NOMA-based hybrid satellite-terrestrial relay networks," in *Proc. IEEE Wireless Commun. Netw. Conf. (WCNC)*, Seoul, South Korea, May 2020, pp. 1–6.
[42] P. K. Sharma and D. I. Kim, "Secure 3D mobile UAV relaying for hybrid satellite-terrestrial networks," *IEEE Trans. Wireless Commun.*, vol. 19, no. 4, pp. 2770–2784, Apr. 2020.
[43] V. Bankey and P. K. Upadhyay, "Physical layer security of multiuser multirelay hybrid satellite-terrestrial relay networks," *IEEE Trans. Veh. Technol.*, vol. 68, no. 3, pp. 2488–2501, Mar. 2019.
[44] K. Guo, K. An, B. Zhang, Y. Huang, and D. Guo, "Physical layer security for hybrid satellite terrestrial relay networks with joint relay selection and user scheduling," *IEEE Access*, vol. 6, pp. 55815–55827, 2018.
[45] I. S. Gradshteyn and I. M. Ryzhik, *Table of Integrals, Series, and Products*. San Diego, CA, USA: Academic, 2000.

HONG-NHU NGUYEN was born in Tien Giang, Vietnam, in March 1971. He received the B.Sc. degree in electronics engineering from the Ho Chi Minh City University of Technology, in 1998, and the M.Sc. degree in electronics engineering from the University of Transport and Communications, Vietnam, in 2012. He is currently pursuing the Ph.D. degree with the Technical University of Ostrava, Czech Republic. He is currently working as a Lecturer with Sai Gon University. His research interests include applied electronics, wireless communication, cognitive radio, energy harvesting.

NGOC-LONG NGUYEN was born in Binh Dinh, Vietnam, in August 1973. He received the B.S. and M.S. degrees in electric physics from the University of Science, Vietnam. He is currently pursuing the Ph.D. degree with the Technical University of Ostrava, Czech Republic. He is currently working as a Lecturer with the Faculty of Applied Sciences, Ton Duc Thang University. His research interests include applied electronics, wireless communication, NOMA cognitive radio, and energy harvesting.

NHAT-TIEN NGUYEN was born in Ho Chi Minh City, Vietnam, in 1981. He received the B.Eng. degree from the Posts and Telecommunications Institute of Technology, in 2011, and the M.Eng. degree from the Ho Chi Minh City University of Technology, in 2017, all in electrical engineering and telecommunications. He is currently pursuing the Ph.D. degree with the Technical University of Ostrava, Czech Republic. He is currently a Lecturer with Sai Gon University. His research interests include applied electronics, wireless communication, cognitive radio, and energy harvesting.

ANH-TU LE was born in Lam Dong, Vietnam, in 1997. He is currently pursuing the Ph.D. degree in communication and information system in the field of wireless communication. He is currently a Research Assistant with the WICOM Lab which was led by Dr. Thuan. He has authored or coauthored over five technical articles published in peer-reviewed international journals. His research interests include the wireless channel modeling, NOMA, cognitive radio, and MIMO.

NHAT-DUY XUAN HA was born in Gia Lai, Vietnam, in 1996. He is currently pursuing the Ph.D. degree in communication and information system in the field of wireless communication. He is currently a Research Assistant with the WICOM Lab which was led by Dr. Thuan. His research interests include the wireless communications, NOMA, cognitive radio, and satellite systems.

DINH-THUAN DO (Senior Member, IEEE) received the B.S., M.Eng., and Ph.D. degrees from Viet Nam National University (VNU-HCMC), in 2003, 2007, and 2013 respectively, all in communications engineering. He was a Visiting Ph.D. Student with the Communications Engineering Institute, National Tsing Hua University, Taiwan, from 2009 to 2010. Prior to joining Ton Duc Thang University, he was a Senior Engineer with the VinaPhone Mobile Network, from 2003 to 2009. He was a recipient of Golden Globe Award from the Vietnam Ministry of Science and Technology, in 2015 (Top 10 talent young scientist in Vietnam). He got Creative Young Medal in 2015. He published one book and five book chapters. He has authored or coauthored over 85 technical articles published in peer-reviewed international journals (SCIE) and over 60 conference papers. He led as a lead guest editor in several special issues in peer-reviewed journals. He serves as Associate Editor in seven ISI/Scopus journals. His research interests include signal processing in wireless communications networks, MIMO, NOMA, UAV networks, satellite systems, physical layer security, device-to-device transmission, and energy harvesting.

MIROSLAV VOZNAK (Senior Member, IEEE) received the Ph.D. degree in telecommunications from the Faculty of Electrical Engineering and Computer Science, VSB-Technical University of Ostrava, in 2002, and the Habilitation degree, in 2009. He was appointed as a Full Professor in electronics and communications technologies, in 2017. His research interests generally focus on information and communication technologies, especially on quality of service and experience, network security, wireless networks, and big data analytics. He is the author or coauthor of more than 100 articles in SCI/SCIE journals. He has served as a member of editorial boards for several journals, including *Sensors, Journal of Communications, Elektronika Ir Elektrotechnika,* and *Advances in Electrical and Electronic Engineering*.